Critical spatially varying earthquake load models for extended structures

A.M. Abbas & C.S. Manohar

Department of Civil Engineering, Indian Institute of Science, Bangalore 560012, India

Synopsis

The problem of modeling spatially varying earthquake loads within the framework of the critical excitation method and finite element modeling of structures is considered. Both deterministic and probabilistic frameworks are considered for modeling the earthquake inputs. In the deterministic analysis, the information available on each component of the support motions is assumed to be limited to the estimates of total energy in the signal, peak values of ground acceleration, velocity and displacement, and an estimate of upper and lower bounds on the Fourier amplitude spectra. The elements of the ground motion vector are represented in terms of modulated Fourier series with undetermined coefficients. These coefficients are optimally determined so that the resulting excitation vector possesses all the known features of the input and, at the same time, produce the highest response in the given structure. Similarly, in the stochastic analysis, the inputs at the support points of the structure are taken to constitute a vector of nonstationary random processes with zero mean. Each of these nonstationary random processes is modeled as a product of a known deterministic envelope function and a stationary Gaussian random process. The auto-power spectral density (psd) functions of the stationary components of the excitations are assumed to be known while the cross-psd functions, that encapsulate spatial variability characteristics of the earthquake loads, are taken to be unknowns. These unknown functions are optimally determined such that the highest response variance of a given structure is maximized under constraints on mathematically permissible variations in the coherency functions. The information on known features of earthquake inputs, for both deterministic and stochastic models, are derived based on the analysis of a set of recorded ground motions. Illustrative examples with reference to an idealized model of a two-span bridge structure, are presented.

Key words: critical seismic excitations; random vibration; spatial variability; extended structures

Critical spatially varying earthquake load models for extended structures

A.M. Abbas[1] & C.S. Manohar[2]

Department of Civil Engineering, Indian Institute of Science, Bangalore 560012, India

Synopsis

The problem of modeling spatially varying earthquake loads within the framework of the critical excitation method and finite element modeling of structures is considered. Both deterministic and probabilistic frameworks are considered for modeling the earthquake inputs. In the deterministic analysis, the information available on each component of the support motions is assumed to be limited to the estimates of total energy in the signal, peak values of ground acceleration, velocity and displacement, and an estimate of upper and lower bounds on the Fourier amplitude spectra. The elements of the ground motion vector are represented in terms of modulated Fourier series with undetermined coefficients. These coefficients are optimally determined so that the resulting excitation vector possesses all the known features of the input and, at the same time, produce the highest response in the given structure. Similarly, in the stochastic analysis, the inputs at the support points of the structure are taken to constitute a vector of nonstationary random processes with zero mean. Each of these nonstationary random processes is modeled as a product of a known deterministic envelope function and a stationary Gaussian random process. The auto-power spectral density (psd) functions of the stationary components of the excitations are assumed to be known while the cross-psd functions, that encapsulate spatial variability characteristics of the earthquake loads, are taken to be unknowns. These unknown functions are optimally determined such that the highest response variance of a given structure is maximized under constraints on mathematically permissible variations in the coherency functions. The information on known features of earthquake inputs, for both deterministic and stochastic models, are derived based on the analysis of a set of recorded ground motions. Illustrative examples with reference to an idealized model of a two-span bridge structure, are presented.

1 INTRODUCTION

Earthquake accelerations are multi-component in nature and these components display both temporal and spatial variations. The temporal variations in earthquake load components have been widely studied. Thus, the response spectrum based approaches for aseismic engineering design effectively take into account the temporal variations in components of earthquake loads *via* modal domain representations. For structures such as chimneys, towers and multi-storied buildings, the lateral structural dimensions are often small in relation to the characteristic seismic wave lengths. Therefore, for this class of structures, the spatial variability of earthquake ground motions are considered to be unimportant. On the other hand, in dealing with long-span land based structures such as, bridges, pipelines and large dams, the differential nature of the earthquake accelerations arising out of spatial variability of ground motions needs to be systematically taken care of. This, in turn, places additional demands on the detail to which the earthquake loads need to be specified for design purposes. Furthermore, the response of the structure here would consist of a pseudo-static component and a dynamic component which need to be separately described.

Given the vast diversity of ground structure and complexity of seismic wave types traveling through the ground, characterizing spatial variability of earthquake ground motions for engineering purposes, becomes a difficult problem. In the existing literature, two alternative approaches have been investigated. In the first approach, one constructs spatial variability models based on statistical processing of ground motion data acquired from strong motion accelerograph arrays that are currently available at a limited number of locations on the earth surface; see, for example, the papers by Loh,[1] Harichandran and Vanmarcke,[2] Luco

[1]Doctoral Candidate, abbas@civil.iisc.ernet.in

[2]Associate Professor, manohar@civil.iisc.ernet.in

and Wong[3] and Abrahamson *et al.*,.[5] In the second alternative, concepts from seismic wave propagation through earth medium are employed to formulate idealized mathematical models for loss of coherency and phase difference effects in ground motions. Thus, the paper by Der Kiureghian[6] proposes a theoretical model for coherency function describing spatial variability of earthquake ground motions. The model consists of three components characterizing three distinct effects of spatial variability, namely, the incoherence effect that arises from scattering of waves in the heterogeneous medium of the ground and their differential superpositioning when arriving from an extended source, the wave passage effect that arises from difference in the arrival times of waves at different stations, and the site-response effect that arises from difference in local soil conditions at different stations. The validation of such theoretical models still, however, requires access to data recorded from strong ground motions or data generated in field studies involving explosion induced ground vibrations. The special issue of the journal, *Structural Safety*,[7] dedicated to the topic of spatial variability of earthquake ground motion, covers wide ranging themes that include: empirical findings from strong motion arrays, ground motion models that incorporate spatial variation; local-soil and kinematic effects due to spatially varying seismic inputs to the foundations; seismic input for lifeline system analysis; design criteria accounting for spatial variations; dense array configurations and data processing from seismological and engineering viewpoints. Discussions on seismic response of structures to spatially varying support motions have also been widely studied; see, for example, the works of Harichandran and Wang,[8,9] Zerva,[10] Der Kiureghian and Neuenhofer,[11] and Zavoni and Vanmarcke.[12]

In this context, it is of interest to note that the availability of strong motion seismic arrays across the earth is presently limited and, has not, in any case, provided adequate data to generate mathematical models that are applicable across wide varieties of spatially changing ground structures. Similarly, in the context of analysis of multi-supported secondary structures in industrial installations, the designer often has access to only the floor response spectrum with no information on the coherency and phase functions that reflect the spatial variability of support motions in the supporting primary structure. While it is a straightforward exercise to generate such information from a random vibration analysis of the primary structure, the results obtained are likely to be strongly influenced by details of model reduction strategies obtained in modeling the primary structure. Thus, when stick models are employed to model the primary systems, as is widely done in the context of nuclear power plant structures, the accuracy with which coherency and phase functions of the floor responses are modeled is open to question. The method of critical excitations, that aims to establish optimal spatial variability characteristics that produces highest response in a given engineering structure, thus, provides valuable alternative perspectives in aseismic design of multi-supported structures. It is of interest to note that except for the studies by Sarkar and Manohar,[13,14] there exists hardly any other investigations into the nature of critical earthquake excitation models for spatially varying ground motions. While, these two studies deal with modeling of spatially varying ground motion within the framework of probabilistic analysis, to the best of authors' knowledge, there has been no studies on modeling of critical earthquake loads for multi-supported structures within the framework of deterministic analysis. The study conducted in this paper aims to gain insights into the nature of critical spatial variability of earthquake ground motions. Specifically, the following points are covered in this study:

1. The deterministic critical excitation modeling approach, as has been developed in a recent work by the present authors,[15] is extended herein to cover multi-supported structures subjected to differential support motions. In this case, each ground acceleration component is modeled as a product of an envelope function and a Fourier series with undetermined coefficients. The envelope functions are taken to be known, while the coefficients of the Fourier series are computed such that the structure response is maximized, subjected to constraints on total energy, peak values of ground acceleration, velocity and displacement, and upper and lower bounds on the Fourier amplitude spectra for the ground motion at each support. The resulting nonlinear optimization problem is solved using sequential quadratic programming.

2. The earlier studies by Sarkar and Manohar[13,14] on stochastic vector critical excitation models were

limited to earthquake loads that were modeled as *stationary* random processes in time. Furthermore, these studies were essentially based on analytical models for structural systems. In the present study, the earlier formulation of these authors is reformulated within the framework of finite element method. Also, the ground motions are now treated as a vector of partially specified *nonstationary* Gaussian random processes. The ground acceleration at each support is obtained by multiplying a deterministic envelope function with a stationary Gaussian random process of zero mean. The envelope functions are assumed to be known while the optimal psd matrix of the stationary part of excitations is obtained such that the structure response variance is maximized under constraints on mathematically permissible lower and upper bounds on the amplitude of cross-psd functions.

3. The response of multi-supported structures subjected to differential support motion is made up of a pseudo-static component and a dynamic component. The determination of these individual components of the response is essential in engineering design. The pseudo-static component of the response here essentially arises because of spatial variability of support motions. Keeping this in mind, the deterministic and probabilistic critical excitation models mentioned above, are formulated in such a way that the critical response variable could either be the pseudo-static component or the dynamic component of the response.

The determination of critical spatially varying earthquake loads is presented with reference to a two-span bridge structure subjected to differential earthquake support motions.

2 MODEL I: DETERMINISTIC CRITICAL EARTHQUAKE LOADS

The equations of motion for a discretized N-degree-of-freedom linear system subjected to $N_{\rm g}$ support motions can be given in a matrix form as follows[16]

$$\begin{bmatrix} \mathbf{M} & \mathbf{M}_{\rm g} \\ \mathbf{M}_{\rm g}^t & \mathbf{M}_{\rm gg} \end{bmatrix} \begin{bmatrix} \ddot{\mathbf{u}}^{tot} \\ \ddot{\mathbf{u}}_{\rm g} \end{bmatrix} + \begin{bmatrix} \mathbf{C} & \mathbf{C}_{\rm g} \\ \mathbf{C}_{\rm g}^t & \mathbf{C}_{\rm gg} \end{bmatrix} \begin{bmatrix} \dot{\mathbf{u}}^{tot} \\ \dot{\mathbf{u}}_{\rm g} \end{bmatrix} + \begin{bmatrix} \mathbf{K} & \mathbf{K}_{\rm g} \\ \mathbf{K}_{\rm g}^t & \mathbf{K}_{\rm gg} \end{bmatrix} \begin{bmatrix} \mathbf{u}^{tot} \\ \mathbf{u}_{\rm g} \end{bmatrix} = \begin{bmatrix} \mathbf{0} \\ \mathbf{P}_{\rm g} \end{bmatrix} \tag{1}$$

Here, $\mathbf{u}^{tot} = [u_1^{tot}, u_2^{tot}, \ldots, u_N^{tot}]^t$ is the N-vector of total displacements at the unconstrained degrees of freedom, $\mathbf{u}_{\rm g} = [u_{\rm g_1}, u_{\rm g_2}, \ldots, u_{\rm g_{N_g}}]^t$ is the $N_{\rm g}$-vector of prescribed support displacements, $\mathbf{M}, \mathbf{C}, \mathbf{K}$ are, respectively, the $N \times N$ mass, damping, and stiffness matrices associated with the superstructure degrees of freedom, $\mathbf{M}_{\rm gg}$, $\mathbf{C}_{\rm gg}$, $\mathbf{K}_{\rm gg}$ are, respectively, the $N_{\rm g} \times N_{\rm g}$ matrices associated with the support degrees of freedom, $\mathbf{M}_{\rm g}$, $\mathbf{C}_{\rm g}$, $\mathbf{K}_{\rm g}$ are, respectively, the $N \times N_{\rm g}$ coupling matrices associated with the superstructure and support degrees of freedom, $\mathbf{P}_{\rm g}$ is the $N_{\rm g}$-vector of the reaction forces at the support degrees of freedom and t denotes matrix transpose. The total displacement can be split into a pseudo-static component, $\mathbf{u}_s$, and a dynamic component, $\mathbf{u}$, as $\mathbf{u}^{tot} = \mathbf{u} + \mathbf{u}_s$. Here, the pseudo-static component, $\mathbf{u}_s$, is the solution of equation 1 excluding the inertia and damping terms, and, is given by

$$\mathbf{u}_s = -\mathbf{K}^{-1}\mathbf{K}_{\rm g}\mathbf{u}_{\rm g} = \mathbf{L}\mathbf{u}_{\rm g} \tag{2}$$

where, $\mathbf{L} = -\mathbf{K}^{-1}\mathbf{K}_{\rm g}$ is the $N \times N_{\rm g}$ influence matrix. Substituting $\mathbf{u}^{tot}$ in terms of $\mathbf{u}$ and $\mathbf{u}_s$ into equation 1, it follows that the equation of motion for the dynamic response component is given by

$$\mathbf{M}\ddot{\mathbf{u}}(t) + \mathbf{C}\dot{\mathbf{u}}(t) + \mathbf{K}\mathbf{u}(t) = -(\mathbf{M}\mathbf{L} + \mathbf{M}_{\rm g})\ddot{\mathbf{u}}_{\rm g}(t) - (\mathbf{C}\mathbf{L} + \mathbf{C}_{\rm g})\dot{\mathbf{u}}_{\rm g}(t) \tag{3}$$

It is assumed that the damping matrix is such that the undamped normal modes uncouple the equation of motions with damping terms included. Let ω_i and ζ_i, denote, respectively, the natural frequency and damping ratio of the structure ith mode. Furthermore, let $\phi = [\phi_1, \phi_2, \ldots, \phi_N]$, be the modal matrix that is normalized such that $\phi^t\mathbf{M}\phi = \mathbf{I}$. Using the transformation $\mathbf{u} = \phi\mathbf{q}$ in equation 4, the equation governing the ith generalized displacement coordinate $q_i(t)$ can be shown to be given by

$$\ddot{q}_i(t) + 2\omega_i\zeta_i\dot{q}_i(t) + \omega_i^2 q_i(t) = \sum_{j=1}^{N_{\rm g}} \{\Psi_{ij}\ddot{u}_{{\rm g}j}(t) + \Gamma_{ij}\dot{u}_{{\rm g}j}(t)\} \tag{4}$$

Here, the matrices $\mathbf{\Psi}$ and $\mathbf{\Gamma}$ are in turn expressed as $\mathbf{\Psi} = -\phi^t(\mathbf{ML} + \mathbf{M}_{\rm g})$ and $\mathbf{\Gamma} = -\phi^t(\mathbf{CL} + \mathbf{C}_{\rm g})$. The coefficients Ψ_{ij} and Γ_{ij} thus can be interpreted as the participation factors associated with ith degree of freedom and jth support motion. The participation factors Γ_{ij}, associated with ground velocity, are often not included in many studies that have been reported in the existing literature on multi-supported excitation problems. This is justified based on an assumption that the effect of the term $\sum_{j=1}^{N_{\rm g}} \Gamma_{ij}\dot{u}_{{\rm g}j}(t)$ is considered to be negligible. In the present study, however, such an assumption is not made. Assuming that the system starts from rest, the kth dynamic displacement component, $u_k(t)$, can be shown to be given by

$$u_k(t) = \sum_{i=1}^{N}\sum_{j=1}^{N_{\rm g}}\{\phi_{ki}[\Psi_{ij}\int_0^t h_i(t-\tau)\ddot{u}_{{\rm g}j}(\tau)d\tau + \Gamma_{ij}\int_0^t h_i(t-\tau)\dot{u}_{{\rm g}j}(\tau)d\tau]\} \tag{5}$$

To develop deterministic critical excitation models we begin by representing the jth support acceleration as $\ddot{u}_{{\rm g}j}(t) = e_j(t)\ddot{w}_{{\rm g}j}(t)$; $j = 1, 2, \ldots, N_{\rm g}$. In this model, $e_j(t)$ is the envelope function that imparts desired transient nature to the excitation and, is taken to be given by $e_j(t) = A_{0j}[\exp(-\alpha_j t) - \exp(-\beta_j t)]$; $\beta_j > \alpha_j > 0$; $j = 1, 2, \ldots, N_{\rm g}$. Here α_j and β_j are the envelope parameters that control the nonstationarity trend of the ground acceleration $\ddot{u}_{{\rm g}j}(t)$ and the constants A_{0j} are selected such that $e_j(t)$ has a peak value of unity. The function $\ddot{w}_{{\rm g}j}(t)$ is a steady state function which is represented in a Fourier series as follows

$$\ddot{w}_{{\rm g}j}(t) = \sum_{m=1}^{N_f}[A_{mj}\cos\Omega_m t + B_{mj}\sin\Omega_m t]; \quad j = 1, 2, \ldots, N_{\rm g} \tag{6}$$

The Fourier coefficients, $\{A_{mj}, B_{mj}\}_{m=1}^{N_f}$, $j = 1, 2, \ldots, N_{\rm g}$, are the $2N_f \times N_{\rm g}$ unknown variables to be optimally determined and $\{\Omega_m\}_{m=1}^{N_f}$, are the frequencies included in the series representation. Since the pseudo-static response is given in terms of the support displacements, it is therefore necessary to compute the associated ground displacements as

$$\dot{u}_{{\rm g}j}(t) = e_j(\tau)\sum_{m=1}^{N_f}\int_0^t[A_{mj}\cos\Omega_m\tau + B_{mj}\sin\Omega_m\tau]d\tau + C_{1j} \tag{7}$$

$$u_{{\rm g}j}(t) = e_j(\tau)\sum_{m=1}^{N_f}\int_0^t[(t-\tau)A_{mj}\cos\Omega_m\tau + B_{mj}\sin\Omega_m\tau]d\tau + C_{1j}t + C_{2j} \tag{8}$$

To calculate the constants of integrations C_{1j}, and C_{2j}, the following conditions are used, $u_{{\rm g}j}(0) = 0$ and $\lim_{t\to\infty}\dot{u}_{{\rm g}j}(t) \to 0$. This leads to

$$C_{2j} = 0; \quad C_{1j} = -\sum_{m=1}^{N_f}\int_0^\infty e_j(\tau)[A_{mj}\cos\Omega_m\tau + B_{mj}\sin\Omega_m\tau]d\tau \tag{9}$$

The problem of determining critical excitation models consists of finding the coefficients $\{A_{mj},\ B_{mj}\}_{m=1}^{N_f}$, $j = 1, 2, \ldots, N_{\rm g}$, such that a specified response variable is maximized subject to a set of constraints that reflect known characteristics of a future earthquake. In the present study, in arriving at these constraints, it is assumed that the information on energy, E_{1j}, peak values of ground acceleration (PGA), M_{1j}, velocity (PGV), M_{2j}, and displacement (PGD), M_{3j}, and upper and lower bounds on the Fourier amplitude spectra (UBFAS & LBFAS), $M_{4j}(\omega)$, $M_{5j}(\omega)$ for $j = 1, 2, \ldots, N_{\rm g}$, are known. This enables the formulation of the following constraints

$$\begin{aligned}&[\int_0^\infty \ddot{u}_{{\rm g}j}^2(t)dt]^{1/2} \le E_{1j}; \quad \max_{0<t<\infty}|\ddot{u}_{{\rm g}j}(t)| \le M_{1j}; \quad \max_{0<t<\infty}|\dot{u}_{{\rm g}j}(t)| \le M_{2j};\\ &\max_{0<t<\infty}|u_{{\rm g}j}(t)| \le M_{3j}; \quad M_{5j}(\omega) \le |\ddot{U}_{{\rm g}j}(\omega)| \le M_{4j}(\omega); \quad j = 1, 2, \ldots, N_{\rm g}\end{aligned} \tag{10}$$

Here, $\ddot{U}_{gj}(\omega)$ is the Fourier transformation of $\ddot{u}_{gj}(t)$. Again, as in the earlier study by Abbas and Manohar,[15] it is proposed that the numerical values for the quantities E_{1j}, M_{1j}, M_{2j}, M_{3j}, $M_{4j}(\omega)$, and $M_{5j}(\omega)$, $j = 1, 2, \ldots, N_g$, be established by using available recorded ground motions. However, it is important to note that, when spatial variability characteristics are included, quantifying these constraints is not as easy as has been the case in singly supported structures. The factors that one has to bear in mind, in this context, are as follows:

1. The spatial extent of the structure.
2. Whether the structure is discretely connected to the ground (as in long-span bridge structures) or is supported continuously (as in large earth dams).
3. The ground conditions at various support points and in the intervening region between the supports. This includes the local soil conditions and depth to the bedrock at the supports.
4. Orientation of the structure with respect to the dominant direction of seismic wave propagation.

To quantify the constraints, it is assumed that a set of ground motion $\{\ddot{v}_{gmj}(t)\}_{m=1}^{N_r}$, $j = 1, 2, \ldots, N_g$, that has been recorded in the past at the site under consideration or other sites with similar soil conditions is available. The quantities E_{1j}, M_{1j}, M_{2j} and M_{3j}, $j = 1, 2, \ldots, N_g$, are computed from this set of past records. Subsequently, this set is normalized such that all records produce a PGA of unity. The upper and lower bound Fourier amplitude spectra for ground acceleration at the jth support are computed through the following equations

$$M_{4j}(\omega) = M_{1j} \max_{1 \le m \le N_r} |\ddot{\bar{V}}_{gmj}(\omega)|; \quad M_{5j}(\omega) = M_{1j} \min_{1 \le m \le N_r} |\ddot{\bar{V}}_{gmj}(\omega)|; \quad j = 1, 2, \ldots, N_g \tag{11}$$

Here, $\{\ddot{\bar{V}}_{gmj}(\omega)\}_{m=1}^{N_r}$ denote the Fourier transform of the normalized past records, $\{\ddot{\bar{v}}_{gmj}(t)\}_{m=1}^{N_r}$, which are computed using the FFT algorithm. Although extensive database on ground motion at various sites having different soil conditions is currently available, the fact still remains that data on spatial variability characteristics is considerably more limited especially as a function of ground variability characteristics. In the Indian continent, for instance, there hardly exist any strong motion data on length scales comparable to the spatial extent of large engineering structures. Given these limitations, to proceed further, we make the following assumptions:

- Attention is focussed only on structures that are discretely supported.
- Depending on local soil conditions at each of the supports, the constraints on ground motion at these supports are derived from database appropriate to the given local soil conditions. Thus, for example, a structure with two support points, with one support on firm soil and, the other on hard soil, two different sets of databases, one applicable to firm soil and other applicable for hard soil are required in deriving the constraints on the critical excitation.
- No constraints are imposed which specifically reflect the nature of ground medium between the intervening supports.

As has been noted already, the response of multi-supported structures subjected to differential support motions consists of a dynamic component and a pseudo-static component. Accordingly, the problems of determining critical excitations for these two response components are considered separately.

Considering the dynamic response to be the response variable of interest, the problem of determining the critical excitation can now be stated as finding $\{A_{mj}, B_{mj}\}_{m=1}^{N_f}$, $j = 1, 2, \ldots, N_g$, that maximize

$$\max_{0<t<\infty} |u_k(t)| = \max_{0<t<\infty} |\sum_{j=1}^{N_g} \sum_{m=1}^{N_f} \phi_{kj} \{\Psi_{jm} \int_0^t e_j(\tau)[A_{mj} \cos \Omega_m \tau + B_{mj} \sin \Omega_m \tau] h_j(t-\tau) d\tau +$$

$$\Gamma_{jm} e_j(t) \int_0^t [A_{mj} \cos \Omega_m \tau + B_{mj} \sin \Omega_m \tau] h_j(t-\tau) d\tau$$
$$-t \int_0^\infty e_j(t) [A_{mj} \cos \Omega_m \tau + B_{mj} \sin \Omega_m \tau] h_j(t-\tau) d\tau \} | \qquad (12)$$

subjected to the constraints listed in equations 10. It is to be emphasized that the objective function here consists of maximization with respect to $\{A_{mj}, B_{mj}\}_{m=1}^{N_f}$, $j = 1, 2, \ldots, N_{\rm g}$ of the maximum response over time. Since, the time at which the dynamic response reaches its maximum value is not known, the solution to this constrained nonlinear optimization problem is carried out at each discrete point of time by using sequential quadratic programming. This results in a family of optimal $\{A_{mj}, B_{mj}\}_{m=1}^{N_f}$, $j = 1, 2, \ldots, N_{\rm g}$ among which, the one that produces the maximum response is taken to define the critical input. Furthermore, the steps of the maximization procedure can be summarized as follows

1. Discretize the time interval of interest, $(0, T_d)$, into discrete instants $t_1, t_2, \ldots, t_f$.
2. Fix $t = t_l$ and compute the impulse response functions, $\{h_i(t_l - \tau)\}_{i=1}^{N}$, $0 \le \tau \le t_l$.
3. Compute $\{A_{mj}, B_{mj}\}_{m=1}^{N_f}$, $j = 1, 2, \ldots, N_{\rm g}$, that maximize the structure dynamic response $u_k(t_l)$ given in equation 5.
4. Repeat steps 2 and 3 for all time points.
5. Estimate the maximum dynamic response $u_{k_{\max}} = \max_{0 \le t_l \le T_d} |u_k(t_l)|$ and record the corresponding optimal $\{A_{mj},\ B_{mj}\}_{m=1}^{N_f}$, $j = 1, 2, \ldots, N_{\rm g}$.
6. The estimated $\{A_{mj}, B_{mj}\}_{m=1}^{N_f}$ define the critical inputs (equations 6 to 8) and the corresponding dynamic response time history (equation 5).

It may be noted that critical excitations that maximize the pseudo-static response component can also be formulated in a similar manner; the relevant details of this formulation are available in the thesis by Abbas.[17]

3 MODEL II: PROBABILSITIC CRITICAL EARTHQUAKE LOADS

In this model, the ground accelerations at the structure supports are modeled as a vector of partially specified nonstationary Gaussian random processes of zero mean. The jth component of this vector is further taken to be of the form $\ddot{u}_{{\rm g}j}(t) = e_j(t) \ddot{w}_{{\rm g}j}(t)$, where $e_j(t)$ is a known deterministic envelope function, as has been given in section 2, and $\ddot{w}_{{\rm g}j}(t)$ is a stationary Gaussian random process of zero mean. The random processes $\ddot{w}_{{\rm g}j}(t)$, $j = 1, 2, \ldots, N_{\rm g}$, can be completely described in terms of the matrix of psd functions $\mathbf{S}(\omega)$. The diagonal term of this matrix, $S_{jj}(\omega)$, represents the auto-psd function of the jth component $\ddot{w}_{{\rm g}j}(t)$. The off-diagonal term $S_{jl}(\omega)$, represents the cross-psd function between $\ddot{w}_{{\rm g}j}(t)$ and $\ddot{w}_{{\rm g}l}(t)$. As is well known, the auto-psd functions are real valued, whereas, cross-psd functions are, in general, complex quantities. Furthermore, the cross-psd functions can also be expressed in the polar form

$$S_{jl}(\omega) = |S_{jl}(\omega)| \exp[i \Phi_{jl}(\omega)]; \quad i = \sqrt{-1}; \quad j \ne l = 1, 2, \ldots, N_{\rm g} \qquad (13)$$

where, $|S_{jl}(\omega)|$ and $\Phi_{jl}(\omega)$ are, respectively, the modulus of the cross-psd function and the phase angle of the ground accelerations at the supports j and l. It is also customary to define the nondimensional coherency function $\gamma_{jl}(\omega)$ given by

$$\gamma_{jl}(\omega) = \frac{|S_{jl}(\omega)|}{\sqrt{S_{jj}(\omega) S_{ll}(\omega)}} \exp[i \Phi_{jl}(\omega)] = |\gamma_{jl}(\omega)| \ \ \exp[i \Phi_{jl}(\omega)]; \quad j \ne l = 1, 2, \ldots, N_{\rm g} \qquad (14)$$

Mathematically, it can be shown that $0 \leq |\gamma_{jl}(\omega)| \leq 1$, with the limit $|\gamma_{jl}(\omega)| = 0$ representing the case of $\ddot{w}_{gj}(t)$ and $\ddot{w}_{gl}(t)$ being uncorrelated, whereas, the other limit, $|\gamma_{jl}(\omega)| = 1$, representing the case where $\ddot{w}_{gj}(t)$ and $\ddot{w}_{gl}(t)$ are fully correlated. It is to be noted that the spatial variability characteristics of the ground motion is reflected through the conditions $S_{jj}(\omega) \neq S_{ll}(\omega)$, $j \neq l = 1, 2, \ldots, N_g$, and, also through the details of spectral variation of $\gamma_{jl}(\omega)$ and $\Phi_{jl}(\omega)$. Thus, in the absence of spatial variability, it turns out that $S_{jj}(\omega) = S_{ll}(\omega)$, $|\gamma_{jl}(\omega)| = 1$ and $\Phi_{jl}(\omega) = 0$ for all $j \neq l = 1, 2, \ldots, N_g$.

The problem of determining critical earthquake load models for spatially varying ground motion can be viewed as finding the elements of the psd matrix $\mathbf{S}(\omega)$ such that a suitable measure of response of the structure is maximized subject to the set of constraints that reflect known characteristics of ground motion. In the present study, we limit our attention in determining the optimal spatial variability characteristics of the ground motion that are encapsulated in the details of $\gamma_{jl}(\omega)$ and $\Phi_{jl}(\omega)$. Consequently, we make the assumption that the knowledge of auto-psd functions $\{S_{jj}(\omega)\}_{j=1}^{N_g}$, is completely available. As in the deterministic critical excitation model, the objective function here is taken to be the highest variance of either the pseudo-static component or the dynamic component of a specified structural response. We begin by focusing our attention on the kth dynamic displacement degree of freedom $u_k(t)$. Using equation 5, the expression for the time history of response variance is obtained by using standard random vibration theory and can be shown to be given by

$$\begin{aligned}\sigma^2_{u_k}(t) = \sum_{i=1}^{N_g}\sum_{j=1}^{N_g}\sum_{m=1}^{N}\sum_{n=1}^{N}\phi_{km}\phi_{kn}\{\Psi_{mi}\Psi_{nj}\int_0^t\int_0^t h_m(t-\tau_1)h_n(t-\tau_2) < \ddot{u}_{gi}(\tau_1)\ddot{u}_{gj}(\tau_2) > d\tau_1 d\tau_2 \\ +\Psi_{mi}\Gamma_{nj}\int_0^t\int_0^t h_m(t-\tau_1)h_n(t-\tau_2) < \ddot{u}_{gi}(\tau_1)\dot{u}_{gj}(\tau_2) > d\tau_1 d\tau_2 + \\ \Gamma_{mi}\Psi_{nj}\int_0^t\int_0^t h_m(t-\tau_1)h_n(t-\tau_2) < \dot{u}_{gi}(\tau_1)\dot{u}_{gj}(\tau_2) > d\tau_1 d\tau_2 + \\ \Gamma_{mi}\Gamma_{nj}\int_0^t\int_0^t h_m(t-\tau_1)h_n(t-\tau_2) < u_{gi}(\tau_1)u_{gj}(\tau_2) > d\tau_1 d\tau_2\} \qquad (15)\end{aligned}$$

In terms of the representation $\ddot{u}_{gj}(t) = e_j(t)\ddot{w}_{gj}(t)$, the expectations appearing in the right hand side of the above equation can be easily evaluated using standard random process calculus, see the thesis by Abbas[17] for the details. Furthermore, it can be shown that

$$\sigma^2_{u_k}(t) = \int_0^\infty \{\sum_{j=1}^{N_g} S_{jj}(\omega)H^d_{kjj}(\omega,t) + \sum_{j=1}^{N_g}\sum_{l=1}^{N_g}|S_{jl}(\omega)|H^d_{kjl}[\omega,\Phi_{jl}(\omega),t]\}d\omega; \quad j \neq l = 1,2,\ldots,N_g \qquad (16)$$

Here, the quantities $H^d_{kjj}(\omega,t)$ and $H^d_{kjl}[\omega,\Phi_{jl}(\omega),t]$ can be interpreted as generalized dynamic transfer functions that are given, respectively, by

$$\begin{aligned}H^d_{kjj}(\omega,t) = \sum_{m=1}^{N}\sum_{n=1}^{N}\phi_{km}\phi_{kn}\{\Psi_{mj}\Psi_{nj}[I_{hjmc}(\omega,t)I_{hjnc}(\omega,t) + I_{hjms}(\omega,t)I_{hjns}(\omega,t)] \\ +\Psi_{mj}\Gamma_{nj}[I_{hjmc}(\omega,t)\bar{I}_{hjnc}(\omega,t) + I_{hjms}(\omega,t)\bar{I}_{hjns}(\omega,t) - I_{hn}(t)(I_{hjmc}(\omega,t)I_{ejc}(\omega,\infty) \\ +I_{hjms}(\omega,t)I_{ejs}(\omega,\infty))] + \Gamma_{mj}\Psi_{nj}[\bar{I}_{hjmc}(\omega,t)I_{hjnc}(\omega,t) + \bar{I}_{hjms}(\omega,t)I_{hjns}(\omega,t) \\ -I_{hm}(t)(I_{ejc}(\omega,\infty)I_{hjmc}(\omega,t) + I_{ejs}(\omega,\infty)I_{hjms}(\omega,t))]\Gamma_{mj}\Gamma_{nj}[I_{hm}(t)I_{hn}(t)(I^2_{ejc}(\omega,\infty) \\ +I^2_{ejs}(\omega,\infty)) + \bar{I}_{hjmc}(\omega,t)\bar{I}_{hjnc}(\omega,t) + \bar{I}_{hjms}(\omega,t)\bar{I}_{hjns}(\omega,t) - I_{hm}(t)(I_{ejc}(\omega,\infty)\bar{I}_{hjnc}(\omega,t) \\ +I_{ejs}(\omega,\infty)\bar{I}_{hjns}(\omega,t)) - I_{hn}(t)(\bar{I}_{hjmc}(\omega,t)I_{ejc}(\omega,\infty) + \bar{I}_{hjms}(\omega,t)I_{ejs}(\omega,\infty))]\} \qquad (17)\end{aligned}$$

$$H^d_{kjl}[\omega,\Phi_{jl}(\omega),t] = X^d_{kjl}(\omega,t)\cos\Phi_{jl}(\omega) + Y^d_{kjl}(\omega,t)\sin\Phi_{jl}(\omega);$$

$$X^d_{kjl}(\omega,t) = \sum_{m=1}^{N}\sum_{n=1}^{N}\phi_{km}\phi_{kn}\{\Psi_{mj}\Psi_{nl}[I_{hjmc}(\omega,t)I_{hlnc}(\omega,t) + I_{hjms}(\omega,t)I_{hlns}(\omega,t)]$$

$$
\begin{aligned}
&+\Psi_{mj}\Gamma_{nl}[I_{hjmc}(\omega,t)\bar{I}_{hlnc}(\omega,t)+I_{hjms}(\omega,t)\bar{I}_{hlns}(\omega,t)-I_{hm}(t)\\
&(I_{hjmc}(\omega,t)I_{elnc}(\omega,\infty)+I_{hjms}(\omega,t)I_{elns}(\omega,\infty))]+\Gamma_{mj}\Psi_{nl}[\bar{I}_{hjmc}(\omega,t)I_{hlnc}(\omega,t)\\
&+\bar{I}_{hjms}(\omega,t)I_{hlns}(\omega,t)-I_{hn}(t)(I_{ejmc}(\omega,\infty)I_{hlnc}(\omega,t)+I_{ejms}(\omega,\infty)I_{hlns}(\omega,t))]\\
&+\Gamma_{mj}\Gamma_{nl}[I_{hm}(t)I_{hn}(t)(I_{ejc}(\omega,\infty)I_{elc}(\omega,\infty)+I_{ejs}(\omega,\infty)I_{els}(\omega,\infty))+\\
&\bar{I}_{hjmc}(\omega,t)\bar{I}_{hjnc}(\omega,t)+\bar{I}_{hjms}(\omega,t)\bar{I}_{hjns}(\omega,t)-I_{hn}(t)(I_{ejc}(\omega,\infty)\bar{I}_{hjnc}(\omega,t)+\\
&I_{ejs}(\omega,\infty)\bar{I}_{hlns}(\omega,t))-I_{hm}(t)(\bar{I}_{hjmc}(\omega,t)I_{elc}(\omega,\infty)+\bar{I}_{hjms}(\omega,t)I_{els}(\omega,\infty))]\};\\
Y^d_{kjl}(\omega,t)=&\sum_{m=1}^{N}\sum_{n=1}^{N}\phi_{km}\phi_{kn}\{\Psi_{mj}\Psi_{nl}[-I_{hjmc}(\omega,t)I_{hlnc}(\omega,t)+I_{hjms}(\omega,t)I_{hlns}(\omega,t)]+\\
&\Psi_{mj}\Gamma_{nl}[I_{hm}(t)(I_{hjmc}(\omega,t)I_{elns}(\omega,\infty)-I_{hjms}(\omega,t)I_{elns}(\omega,\infty))-I_{hjmc}(\omega,t)\bar{I}_{hlns}(\omega,t)+\\
&I_{hjms}(\omega,t)\bar{I}_{hlnc}(\omega,t)]+\Gamma_{mj}\Psi_{nl}[I_{hn}(t)(I_{ejmc}(\omega,\infty)I_{hlns}(\omega,t)-I_{ejms}(\omega,\infty)I_{hlns}(\omega,t))-\\
&\bar{I}_{hjmc}(\omega,t)I_{hlns}(\omega,t)-\bar{I}_{hjmc}(\omega,t)I_{hlnc}(\omega,t))]+\Gamma_{mj}\Gamma_{nl}[-I_{hm}(t)I_{hn}(t)(I_{ejc}(\omega,\infty)I_{els}(\omega,\infty)-\\
&I_{ejs}(\omega,\infty)I_{elc}(\omega,\infty))-\bar{I}_{hjmc}(\omega,t)\bar{I}_{hjns}(\omega,t)+\bar{I}_{hjms}(\omega,t)\bar{I}_{hjnc}(\omega,t)+I_{hn}(t)(I_{ejc}(\omega,\infty)\bar{I}_{hlnc}(\omega,t)\\
&-I_{ejs}(\omega,\infty)\bar{I}_{hlnc}(\omega,t))+I_{hm}(t)(\bar{I}_{hjmc}(\omega,t)I_{elc}(\omega,\infty)-\bar{I}_{hjms}(\omega,t)\bar{I}_{elc}(\omega,\infty))]\}
\end{aligned}
\tag{18}
$$

where

$$
\begin{aligned}
I_{hjmc}(\omega,t)&=\int_0^t h_m(t-\tau)\cos\omega\tau\; e_j(\tau)d\tau;\;\; I_{hjms}(\omega,t)=\int_0^t h_m(t-\tau)\sin\omega\tau\; e_j(\tau)d\tau\\
I_{ejc}(\omega,\infty)&=\int_0^\infty e_j(\tau)\cos\omega\tau d\tau;\;\; I_{ejs}(\omega,\infty)=\int_0^\infty e_j(\tau)\sin\omega\tau d\tau;\;\; I_{hm}(t)=\int_0^t h_m(t-\tau)d\tau\\
\bar{I}_{hjmc}(\omega,t)&=\int_0^t h_m(t-\tau)I_{ejc}(\omega,\tau)d\tau;\;\; \bar{I}_{hjms}(\omega,t)=\int_0^t h_m(t-\tau)I_{ejs}(\omega,\tau)d\tau
\end{aligned}
\tag{19}
$$

Expressions for $I_{hlnc}(\omega,t)$, $I_{hlns}(\omega,t)$, $I_{elc}(\omega,\infty)$, $I_{els}(\omega,\infty)$, $\bar{I}_{hlnc}(\omega,t)$, $\bar{I}_{hlns}(\omega,t)$ and $I_{hn}(t)$ can be computed from the above equation after replacing j and m by l and n, respectively. It is important to note here some of the features of the functions $\{H^d_{kjj}(\omega,t)\}_{j=1}^{N_g}$ and $\{H^d_{kjl}[\omega,\Phi_{jl}(\omega),t]\}_{j\neq l=1}^{N_g}$ appearing in equation 16. While the functions $\{H^d_{kjj}(\omega,t)\}_{j=1}^{N_g}$ are nonnegative, the functions $\{H^d_{kjl}[\omega,\Phi_{jl}(\omega),t]\}_{j\neq l=1}^{N_g}$ can take either positive or negative values depending on the nature of the phase angles $\{\Phi_{jl}(\omega)\}_{j\neq l=1}^{N_g}$. For instance, we consider the structure response under the single ground motion $\ddot{u}_{gj}(t)$ for $j=1$ with other excitations $\ddot{u}_{gj}(t)=0$, for $j=2,3,\ldots,N_g$. In this case, the structure dynamic response variance is given by the first term $\int_0^\infty S_{11}(\omega)H^d_{k11}(\omega,t)d\omega$ of equation 16. Furthermore, let $t=t^*$, $\omega=\omega^*$ and consider $\ddot{w}_{g1}(t)$ to be a narrow band random process with its psd function $S_{11}(\omega)$ that has a central frequency located at $\omega=\omega^*$. Since $S_{11}(\omega^*)$ is a nonnegative quantity, and for $\sigma^2_{\dot{u}_k}(t^*)$ to be positive, it follows that $H^d_{k11}(\omega^*,t^*)$ must be positive. This is true for all values of $\omega=\omega^*$ and $t=t^*$. Following this argument, it can be shown that $\{H^d_{kjj}(\omega,t)\}_{j=2}^{N_g}$ are also nonnegative functions. On the other hand, the fact that $\{H^d_{kjl}[\omega,\Phi_{jl}(\omega),t]\}_{j\neq l=1}^{N_g}$ can take both positive and negative values can easily be verified by noting the presence of trigonometric terms in equation 18. It may be emphasized also that the functions $\{H^d_{kjj}(\omega,t)\}_{j=1}^{N_g}$ and $\{H^d_{kjl}[\omega,\Phi_{jl}(\omega),t]\}_{j\neq l=1}^{N_g}$ are dependent not only on the system characteristics but also on time as well. Additionally, the functions $\{H^d_{kjl}[\omega,\Phi_{jl}(\omega),t]\}_{j\neq l=1}^{N_g}$ are dependent on some of the excitation characteristics. These functions require careful interpretation since they do not possess some of the well known characteristics of the classical frequency response functions. For instance, it is not appropriate to consider their inverse Fourier transforms, since, such transforms do not permit the usual interpretation of being the system impulse response functions.

As per the definition of critical excitation models employed in this study, the problem of computing optimal ground motion consists of determining $\{S_{jl}(\omega)\}_{j\neq l=1}^{N_g}$ that maximizes $\max_{0\leq t\leq\infty}\sigma^2_{\dot{u}_k}(t)$. This optimization has to be carried out under the constraints $0\leq|S_{jl}(\omega)|\leq\sqrt{S_{jj}(\omega)S_{ll}(\omega)}$; $j\neq l=1,2,\ldots,N_g$. This problem again constitutes a constrained nonlinear optimization problem and, in principle, can be

solved using sequential optimization programming after a suitable discretization scheme is adopted to represent $\{\ddot{w}_{gj}(t)\}_{j=1}^{N_g}$. In this study, however, such a numerical approach is found to be not necessary. In fact, the optimal cross-psd functions can easily be written down based on a careful inspection of terms on the right hand side of equation 16. The earlier studies by Sarkar and Manohar,[13,14] in the context of stationary spatially varying ground motion models, recognize this aspect. To proceed further, we consider two alternative scenarios. In the first case, it is assumed that $\{|S_{jl}(\omega)|\}_{j\neq l=1}^{N_g}$ are the only unknowns, while, $\{\Phi_{jl}(\omega)\}_{j\neq l=1}^{N_g}$ remain known. In the second case, it is assumed that the functions $\{S_{jl}(\omega)\}_{j\neq l=1}^{N_g}$ are entirely unknown.

3.1 Critical cross-psd functions with phase known

In this case, we assume that prior knowledge on the phase spectra, $\{\Phi_{jl}(\omega)\}_{j\neq l=1}^{N_g}$, is known while $\{|S_{jl}(\omega)|\}_{j\neq l=1}^{N_g}$ are unknowns. Specifically, we assume that the phase spectra are of the form $\Phi_{jl}(\omega) = \omega\tau_{jl}$, $j \neq l = 1, 2, \ldots, N_g$. Here, $\tau_{jl} = D_{jl}/V$ is the seismic transmission time lag over a span D_{jl} between the two supports j and l, and V is the apparent velocity of propagation. This case is relevant to problems in which:

- the phase differences arise due to the wave passage effect caused by plane waves arriving at a single incident angle at the two stations j and l and
- the contribution to the phase due to the differences in local soil conditions is considered negligible.

Furthermore, this case is considered acceptable for modeling earthquake inputs to long span structures. Consequently, the optimization problem here consists of finding the quantities $\{|S_{jl}(\omega)|\}_{j\neq l=1}^{N_g}$ so that the dynamic response variance,

$$\max_{0<t<\infty} \sigma_{u_k}^2(t) = \max_{0<t<\infty} \int_0^\infty \{\sum_{j=1}^{N_g} S_{jj}(\omega) H_{kjj}^d(\omega, t) + \sum_{j=1}^{N_g}\sum_{l=1}^{N_g} |S_{jl}(\omega)| H_{kjl}^d(\omega, \tau_{jl}, t)\} d\omega;\ j \neq l = 1, 2, \ldots, N_g \quad (20)$$

is maximized subject to lower and upper bounds on these quantities given by $0 \leq |S_{jl}(\omega)| \leq \sqrt{S_{jj}(\omega) S_{ll}(\omega)}$; $j \neq l = 1, 2, \ldots, N_g$. Here, expression for $H_{kjj}^d(\omega, t)$ is as given by equation 17. The expression for $H_{kjl}^d(\omega, \tau_{jl}, t)$ can be obtained from equation 18 after substituting $\Phi_{jl}(\omega) = \omega\tau_{jl}$. Again, it may be observed from equation 16 that, for a given time $t = t^*$, the contribution to the response variance from the terms involving auto-psd functions is always positive, while the contribution from terms involving cross-psd functions is either positive or negative depending on the sign of the functions $H_{kjl}^d(\omega, \tau_{jl}, t^*)$. Thus, it follows that the optimal $\{|S_{jl}(\omega)|\}_{j\neq l=1}^{N_g}$ that produce the highest dynamic response variance, at a fixed time t^*, must be of the form

$$\begin{aligned} |S_{jl}(\omega)| &= 0 \quad \text{if} \quad H_{kjl}^d(\omega, \tau_{jl}, t^*) \leq 0; \\ |S_{jl}(\omega)| &= \sqrt{S_{jj}(\omega) S_{ll}(\omega)} \quad \text{if} \quad H_{kjl}^d(\omega, \tau_{jl}, t^*) > 0; \quad j \neq l = 1, 2, \ldots, N_g \end{aligned} \quad (21)$$

Since, the point at which $\sigma_{u_k}^2(t)$ reaches its maximum value is not known, the solution to this maximization problem is carried out at each discrete point of time as has been done for deterministic models. Thus, the time duration of interest is discretized into steps of Δt. The optimal $\{|S_{jl}(\omega)|\}_{j\neq l=1}^{N_g}$ that maximize the response variance at each discrete point of time are computed. Among this family of optimal $\{|S_{jl}(\omega)|\}_{j\neq l=1}^{N_g}$, the one that produces the maximum response variance is taken to define the critical input. Additionally, the details of the maximization procedure read as

1. Compute the phase spectra, $\Phi_{jl}(\omega) = \omega\tau_{jl}$, $j \neq l = 1, 2, \ldots, N_g$.
2. Discretize the time interval of interest, $(0, T_d)$, into discrete instants $t_1, t_2, \ldots, t_f$.

3. Fix $t = t_i$ and evaluate the functions $H^d_{kjj}(\omega, t_i)$ and $H^d_{kjl}(\omega, \tau_{jl}, t_i)$, $j \neq l = 1, 2, \ldots, N_g$, (equations 17 & 18).

4. Compute the optimal $|S_{jl}(\omega)|$, $j \neq l = 1, 2, \ldots, N_g$ that maximize $\sigma^2_{u_k}(t_i)$, using equations 21 and record the corresponding optimal response variance $\sigma^2_{u_k}(t_i)$.

5. Repeat steps 3 and 4 for all time points.

6. Estimate the maximum dynamic response variance as $\sigma^2_{u_{k\max}} = \max_{0<t<T_d} \sigma^2_{u_k}(t_i)$ and record the corresponding optimal $|S_{jl}(\omega)|$, $j \neq l = 1, 2, \ldots, N_g$.

7. Compute the time history of the critical dynamic response variance (equation 16).

3.2 Critical cross-psd functions with phase unknown

In this section, we consider a more general case in which, in addition to the amplitude of the inputs cross-psd functions, the associated phase spectra are also taken to be unknowns. The diagonal terms of the inputs psd matrix which represent the auto-psd functions are, as before, taken to be known. This situation can be easily conceived, since information from densely spaced strong motion seismic arrays is more scarce than data from single point ground acceleration measurements. Furthermore, this case is relevant to problems of short-span structures based on rapidly varying local soil conditions. Thus, the optimization problem here consists of finding $|S_{jl}(\omega)|$ and $\Phi_{jl}(\omega)$, $j \neq l = 1, 2, \ldots, N_g$, such that the highest dynamic response, given by equation 20, is maximized, subject to the constraints given in the previous section. In order to tackle this problem, it can be noted that, for a fixed time $t = t^*$, the generalized transfer function $H^d_{kjl}[\omega, \Phi_{jl}(\omega), t^*]$ appearing in equation 16 can be rewritten as

$$H^d_{kjl}[\omega, \Phi_{jl}(\omega), t^*] = Z_{jl}(\omega, t^*) \cos[\Phi_{jl}(\omega) - \theta_{jl}(\omega, t^*)]; \quad j \neq l = 1, 2, \ldots, N_g \tag{22}$$

where

$$Z_{jl}(\omega, t^*) = \sqrt{{X^d_{kjl}}^2(\omega, t^*) + {Y^d_{kjl}}^2(\omega, t^*)}; \quad \theta_{jl}(\omega, t^*) = tan^{-1}\{\frac{Y^d_{kjl}(\omega, t^*)}{X^d_{kjl}(\omega, t^*)}\} \tag{23}$$

Therefore, for $\sigma^2_{u_k}(t^*)$ to be maximum, it follows that

$$|S_{jl}(\omega)| = \sqrt{S_{jj}(\omega) S_{ll}(\omega)}; \quad \cos[\Phi_{jl}(\omega) - \theta_{jl}(\omega, t^*)] = 1; \quad j \neq l = 1, 2, \ldots, N_g \tag{24}$$

The second part of the above equation leads to

$$\Phi_{jl}(\omega) = \theta_{jl}(\omega, t^*) = tan^{-1}\{\frac{Y^d_{kjl}(\omega, t^*)}{X^d_{kjl}(\omega, t^*)}\}; \quad j \neq l = 1, 2, \ldots, N_g \tag{25}$$

Consequently, it follows that the maximum response is produced by fully coherent ground motion ($|S_{jl}(\omega)| = \sqrt{S_{jj}(\omega) S_{ll}(\omega)}$), but with phase angles that correspond neither to in phase nor to out of phase ground motions. Again, as has been mentioned in the previous section, the maximization across time is to be carried out at each discrete point of time. The details of the computational steps are similar to those given in the previous section. The problem of determining critical cross-psd functions that maximize the highest variance of the pseudo-static response can also be formulated following steps that are similar to those that have been used for maximizing dynamic response variance. These details, however, are not provided herein.

As has been already mentioned, in the present study, we assume that the knowledge of auto-psd functions $S_{jj}(\omega)$, $j = 1, 2, \ldots, N_g$, is completely available. This would mean that the constraints on total energy, zero crossing rate and entropy rate on individual components of ground motions are not directly

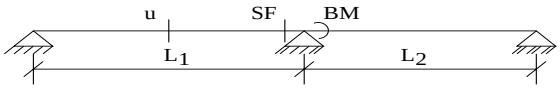

Figure 1: Example structure considered

imposed in the present formulation. These properties, are in fact, assumed to be already encapsulated in the known auto-psd functions. Thus, the issue here is not on determining the optimal average power distribution across the frequency of individual excitation components, but, instead we limit the attention to spatial variability characteristics that are embodied in details of $|S_{jl}(\omega)|$ and $\Phi_{jl}(\omega)$, $j \neq l = 1, 2, \ldots, N_{\rm g}$. It is possible to formulate a more general critical excitation model wherein, all elements of psd matrix are considered as partially specified. Examples of such alternative perspectives on determining stochastic critical excitation models for spatially varying ground motion can be found elsewhere.[17]

4 NUMERICAL ILLUSTRATIONS & DISCUSSIONS

For the purpose of illustrating the formulations developed in sections 2 and 3, a simple two-span bridge idealized as a two-span Euler-Bernoulli beam is considered, see Figure 1. This structure is taken to have a constant mass per unit length, m, and flexural rigidity, EI, with $EI/m = 40.50 \times 10^6 \mathrm{m}^4/\mathrm{s}^2$, $L_1 = 55.00$ m and $L_2 = 45.00$ m.[11] The structure is discretized into forty, 2-noded beam elements, with one translational and one rotational degrees of freedom per node. A free vibration analysis revealed that the first five natural frequencies of the structure are 3.79, 9.70, 14.68, 22.38 and 32.49 Hz, respectively. The highest frequency in the series representation of the excitations is taken to be 25.00 Hz, and the response analysis is carried out by retaining the first four modes. Consequently, it turns out that $N = 4$, while the number of prescribed support motions $N_{\rm g} = 3$. A modal viscous damping of 5 per cent is assumed for all the four modes. The local soil conditions at the three supports are assumed to be identical and correspond to firm soil condition. Each of the supports is taken to be acted upon by one transverse support motion. The structure is analyzed separately for the dynamic and pseudo-static response components. Three response quantities, namely, midpoint displacement of the left span, shear force at the left side of the middle support and bending moment at the middle support are considered as the response variables to be maximized. Critical excitations are computed for the deterministic model of section 2 and the probabilistic model of section 3. Additionally, a third model is also considered. In this model, the ground motions are taken to be deterministic and are assumed to be represented as

$$\ddot{u}_{{\rm g}j}(t) = \sum_{m=1}^{N_r} a_{mj} \ddot{\bar{v}}_{{\rm g}mj}(t); \quad j = 1, 2, \ldots, N_{\rm g} \tag{26}$$

Here, $\{\ddot{\bar{v}}_{{\rm g}mj}(t)\}_{m=1}^{N_r}$, $j = 1, 2, \ldots, N_{\rm g}$, are past recorded ground motions that are normalized to possess unit PGA and recorded on sites with soil conditions that match with the local soil condition at the jth support of the structure, and $\{a_{mj}\}_{n=1}^{N_r}$, $j = 1, 2, \ldots, N_{\rm g}$, are the $3N_r$ unknown optimization variables that are to be determined such that the highest dynamic/pseudo-static response is maximized subjected to the constraints on E_{1j}, M_{1j}, M_{2j} and M_{3j}. Again, this constitutes a constrained nonlinear optimization problem and is solved using the same procedure as has been outlined in section 2. Critical earthquake excitations derived using equation 26 are referred to as Model III in the subsequent discussion. The details of maximization procedure follow the same lines as has been given for model I.

4.1 Description of constraints

The vertical components of a set of ten earthquake records are adopted for quantifying the known information on critical earthquake excitations for both deterministic and probabilistic earthquake load models in the present study.[17] Based on an analysis of these records the following values were selected ($j = 1, 2, 3$),

$E_{1j} = 3.03$ m/s$^{1.5}$, $M_{1j} = 4.10$ m/s^2 (0.42 g), $M_{2j} = 0.21$ m/s, $M_{3j} = 0.14$ m. Figure **??** shows the plots of $M_{4j}(\omega)$ and $M_{5j}(\omega)$, which respectively, are the upper and lower bounds on the Fourier amplitude spectra as defined in equation 19. In the numerical calculations it is assumed that the acceleration frequency range lies in 0.20 to 25.00 Hz. The parameters of the envelope modulation $\{\alpha_j,\ \beta_j\}_{j=1}^3$ and $\{A_{0j}\}_{j=1}^3$ are taken as $\{\alpha_j = 0.13,\ \beta_j = 0.50\}_{j=1}^3$ and $\{A_{0j} = 2.17\}_{j=1}^3$. These, in turn, fix the duration of the critical earthquake to be around 30 s for all the support motions. In deriving the stochastic critical excitations, the auto-psd function at the jth support point, $S_{jj}(\omega)$, is taken to be given by the Kanai-Tajimi psd

$$S_{jj}(\omega) = S_0 \frac{\omega_{gj}^4 + 4\eta_{gj}^4\omega^2\omega_{gj}^2}{(\omega_{gj}^2 - \omega^2)^2 + 4\eta_{gj}^4\omega^2\omega_{gj}^2} \quad \frac{\omega^4}{(\omega_{fj}^2 - \omega^2)^2 + 4\eta_{fj}^2\omega^2\omega_{fj}^2} \tag{27}$$

Here, S_0 is the intensity of the psd function at the rock layer and is taken to be 0.014 m^2/s^3. This value implies that the expected peak ground acceleration at the jth support is about 0.42 g, which is the same value as has been used for the deterministic models. Furthermore, the central frequency of each random process, ω_{gj}, is assumed to be 10.81 rad/s (1.72 Hz), which is selected based on the dominant frequency observed from Fourier analysis of past recorded ground accelerations. The parameters of the filter functions are taken to be $\{\omega_{fj}\}_{j=1}^3 = 1.50$ rad/s (0.24 Hz), and $\{\eta_{fj}\}_{j=1}^3 = 0.60$, that are valid for a firm soil site.[16] For the phase model of section 3.1, the apparent wave velocity, V, is taken to be 500 m/s. This leads to the time lags between the three supports to be $\tau_{12} = 0.11$ s, $\tau_{23} = 0.09$ s and $\tau_{13} = 0.20$ s.

4.2 Numerical results on critical excitations and responses

Before we give the detailed description of the numerical results obtained, it is useful to summarize the various case studies and models that have been investigated. Thus, the numerical results that are obtained encompass the following aspects:

1. Two deterministic models (I & III) and one probabilistic model (model II).
2. Different response variables that include displacement and stress resultant.
3. Dynamic and pseudo-static components of each of the above response variables.
4. Several alternative constraints scenarios for each model.
5. Critical inputs and corresponding structure responses from each model.
6. Structure responses to past recorded ground motions.
7. Coherency functions from existing models and corresponding structure responses.

In the probabilistic model, two different cases are studied depending on whether phase spectra of ground accelerations are taken to be known or unknown. In the deterministic models, the response variables considered include displacement of the left span midpoint, bending moment and shear force at the middle support. Similarly, in the probabilistic model, the response variables are taken to be the variances of these quantities. The nomenclature used for describing various models and the constraints scenarios are summarized in Table 1. The results from the deterministic models include time histories and Fourier spectra of critical accelerations, while results on probabilistic models are illustrated with critical cross-psd functions and critical phase spectra. For the sake of comparing maximum responses from critical models with those from past records, the maximum dynamic and pseudo-static responses were also computed for the structure under the effect of past recorded ground motions. In computing these response, it is assumed that the ground motions propagate from left support towards the middle and right supports with an apparent wave velocity of propagation $V = 500$ m/s. The details on the selection of parameters that reflect convergence criteria for the optimization algorithm, choice of starting solution to initiate the optimization process and choice of specific frequencies to be included in the series representation for the

support motion are made following the criteria that have been mentioned in an earlier study.[15] An analysis for determining the number of frequency terms N_f, for Models I and II showed that around 34 terms give satisfactory results for both the models. Therefore, N_f was taken to be 34 in the subsequent calculations. This means that the total number of optimization variables in model I is 204 and for model III this number is $3N_r = 30$. In order to compare the critical responses computed from the probablistic model with those from existing coherency models, the following three alternative models for coherency functions, as given by equation 14 are considered. The details of these models are provided in reference 17.

A comprehensive parametric study has been conducted covering the aspects described in the previous section. The numerical results here constitute only a subset of the extensive results obtained and it is hoped that the results that are chosen to be included bring out various aspects of the critical inputs and responses. The results on critical earthquake excitations from the deterministic model I, case 4 are presented in Figures 2 to 4. Each of these Figures shows the time history and the corresponding Fourier amplitude spectrum of the critical ground acceleration at one of the structure three support points. Here, the objective function of maximization is taken as the pseudo-static displacement of the left span midpoint. Corresponding maximum responses produced by these critical excitations for alternative dynamic and pseudo-static objective functions are listed in Tables 2 and 3. Results on critical cross-psd functions from the probabilistic model II are illustrated in Figures 5 to 7. Here, critical $|S_{jl}(\omega)|$, $j \neq l = 1, 2, 3$, when phase spectra are taken to be known (case 1) are shown in Figures 5(a) to 7(a) with the response variable taken as the dynamic bending moment at the middle support. Corresponding results when the pseudo-static bending moment at middle support midpoint is taken as the response variable of maximization are presented in Figures 5(b) to 7(b). The results on critical phase spectra of case 2 from model II are given in Figure 8 with dynamic and pseudo-static displacement response at the midpoint of the left span adopted as the response variables of maximization. The corresponding peak values of these responses are summarized in Tables 2 and 3 for alternative objective functions. The estimated coherency functions from deterministic model I are presented in Figures 9 and 10.

4.3 Discussions on numerical results

From a careful study of the results presented in Figures 2 to 9 and Tables 2 and 3, the following observations can be made:

1. In model I, the frequency content of individual ground motion depends upon choice of objective function (dynamic/pseudo-static component) of displacement/stress resultant on nature of constraints imposed. With dynamic response component as the objective function, the dependency of frequency content on alternative constraints scenarios considered (Table 1) broadly resembles those observed for the case of single-point critical excitations.[15] That is, with constraints on total energy, PGA, PGV, UBFAS and LBFAS, the excitation tends to become richer in frequency content than what otherwise is observed with other constraint scenarios. Thus, when no constraints are imposed on Fourier amplitude spectra (case 1 & 2), the excitation tends to be narrow banded while with introduction of these constraints, the excitation tends to become broad band in nature. With dynamic component of bending moment and shear force as objective functions, similar features were observed although these results have not been included in the paper.

2. With pseudo-static component of the response as the objective function, as might be expected, the critical excitations show several new features. Given that the pseudo-static response depends upon ground displacements, it becomes crucial to include constraints on PGD. If constraints on PGD were not to be imposed the resulting critical excitations show unrealistic large ground displacements. Similarly, it was also observed that with no constraints on Fourier amplitude spectra, the spectrum of ground acceleration showed unrealistic features in terms of input energy getting increasingly shifted towards high frequency ends. With the introduction of constraints on PGD and Fourier amplitude spectra, the spectrum of inputs tends to become broad banded and more realistic as may be evidenced from Figures 2 to 4.

3. The nature of critical excitation was seen to be dependent on the response variable adopted as an objective function. This is indicated for model II, case 1, by comparing the amplitude functions in Figures 5(a) to 7(a) where the objective function has been the dynamic component of the bending moment at middle support, with those presented in Figures 5(b) to 7(b) where the pseudo-static component of the bending moment at the same point is the objective function. Similar features were also observed in the deterministic model I although detailed results on this are not included.

4. For probabilistic model, with phase spectra available (case 1), critical responses are produced by coherency functions that neither correspond to fully correlated nor to independent ground motions (see Figure 5 to 7. On the other hand, when phase spectra are not known (case 2), the critical excitations are seen to be fully coherent but the phase spectra reveal system dependent feature which corresponds to neither in phase nor to out of phase motions as can be seen in Figure 8. Also, the maximum critical responses from the probabilistic models are seen to be higher than those from fully correlated inputs, independent inputs or from correlated excitations with established coherency models. For example, the maximum standard deviation of critical displacement is about 1.6 times that from established coherency models and is of the same order compared with maximum value from fully correlated ground motion. Again, the estimated coherency functions from critical excitations of model I, also reveal that these excitations have specific system dependence coherencies that neither correspond to fully correlated ground motion nor to independent ground motions. Comparing coherency and phase spectrum models shown in Figures 9 and 10 (from model I) with similar results shown in Figures 8 (from model II), it follows that the details of spectral variation of critical coherency and phase functions are quite dissimilar for the deterministic and probabilistic models. This points towards the conclusion that the formulation of critical coherency and phase models depends crucially on details of constraints imposed and framework adopted for modeling.

5. The maximum pseudo-static responses from deterministic models (I, case 4 & III, case 2), are seen to compare well, see Tables 2 and 3. These maximum responses (displacement and stress resultant) are around 1.3, 2.0 and 2.0 times those from past records. While, maximum pseudo-static responses produced from deterministic and probabilistic models reveal peak factors of 1.5, 2.2 and 2.3 for displacement, bending moment and shear force, respectively (see Table 3). These peak factors appear to be low, which might be attributed to the fact that, in model II the auto-psd functions of the inputs are described a priory and, hence, are not optimized to produce higher responses. On the other hand, in model I, the Fourier coefficients are treated as variables of optimization, which allow the excitation to distribute its energy around structural resonant frequencies. Similar observation holds good when the objective function is taken as the structure dynamic response component (see Table 2).

6. As has been already mentioned, contrary to current practice, in the computation of critical excitations that maximize the structure dynamic responses, the velocity dependent terms that appear in the right hand side of equation 3 are not ignored. In deterministic model I, the inclusion of these terms in formulating critical excitations was seen to produce dramatic increase in structure responses, especially, when no constraints were imposed on PGV (case 1). With the introduction of these constraints, the structure maximum responses due to velocity dependent excitations was found to be up to 10 per cent. On the other hand, for probabilistic model, the inclusion of these velocity terms (equation 15) was seen to increase the standard deviations of the structure responses by about 7 per cent.

7. For the example structure considered herein, the structure responses are seen to be dominated by pseudo-static effects. This might be attributed to the fact that the structure is relatively stiff and short. This also underlines the importance of considering spatial variability of ground motions for this class of structures.

5 CONCLUSIONS

Given the paucity of recorded ground motions that reflect spatial variability of earthquake ground motions on length scales comparable to typical dimensions of large engineering structures, an attempt has been made in this study to develop critical earthquake excitation models with emphasis placed primarily on spatial variability characteristics of ground motion. In relation to existing literature on this subject, the following aspects of the work are considered to be novel:

- The problem of deriving critical earthquake excitations for multi-supported linear structures is tackled within deterministic and probabilistic frameworks.
- Models I and III of the present study represent new investigations into the nature of deterministic modeling of critical spatially varying earthquake ground motion for multiply supported structures.
- In the probabilistic model, the ground motion which was taken to be represented as a vector of stationary random processes in the earlier studies by Sarkar and Manohar[13, 14] is now modeled as a vector of nonstationary random processes.
- The structural response characterization has been made within the framework of finite element modeling. Thus, although the numerical illustration in the present study is on a simple two-span beam structure, the formulation itself is more widely applicable.

The results obtained from both deterministic and probabilistic critical excitation models have shown many common features. Thus, for example both deterministic model I and probabilistic model with phase known predict that highest responses are produced by system dependent partially coherent ground motions. Similarly, the critical phase spectra are also seen to be system dependent and this spectra correspond neither to perfectly in phase motions nor to perfectly out of phase motions. The deterministic models allow for optimization of not only the spatial variability characteristics but also the spectral distribution of the total energy for the individual support motion. On the other hand, in probabilistic critical excitation models, attention is limited to only those aspects of spatial variability that are encapsulated in the cross-psd functions with the auto-psd functions taken to be known a priory. Although the deterministic and probabilistic critical excitation models share common broad features, the details of the spectral variation of critical coherency and phase functions, on the other hand, are observed to be markedly different for the two models. This points towards sensitivity of critical spatial variation with respect to nature of constraints imposed and framework adopted for modeling. It is of interest to note also that the responses produced by probabilistic critical excitations offer mathematically exact upper bounds on responses of multiply supported linear structures with respect to alternative models for input cross coherency functions.

References

[1] Loh, C., "Analysis of the spatial variation of seismic waves and ground movements from SMART-1 array data", *Earthquake Engineering and Structural Dynamics*, 1985, 13, pp. 561-585.

[2] Harichandran, R.S., Vanmarcke, E.H., "Stochastic variation of earthquake ground motion in space and time", *Journal of Engineering Mechanics*, 1986, 112, pp. 154-174.

[3] Luco, J.E., Wong, H.L., "Response of a rigid foundation to a spatially random ground motion", *Earthquake Engineering and Structural Dynamics*, 1986, 14, pp. 891-908.

[4] Abrahamson, N.A., Bolt, B.A., Darragh, R.B., Penzien, J., and Tsai, Y.B., "The SMART I accelerograph array (1980-1987): A review", *Earthquake Spectra*, 1987, 3, pp. 263-287.

[5] Abrahamson, N.A., Schneider, F.S., and Stepp, C. (1991), "Spatial coherency of shear waves from Lotung, Taiwan large-scale seismic test, *Structural Safety*, **10**, 145-162.

[6] Kiureghian, A.D., "A coherency model for spatially varying ground motions", *Earthquake Engineering and Structural Dynamics*, 1996, 25, pp. 99-111.

[7] Vanmarcke, E.H., "Special issue: Spatial variation of earthquake ground motion", *Structural Safety*, 1991, 9, pp.1-267.

[8] Harichandran, R.S., Wang, W., "Response of simple beam to spatially varying seismic excitation", *Journal of Engineering Mechanics*, 1988, 114, pp. 1526-1541.

[9] Harichandran, R.S., Wang, W., "Response of indeterminate two-span beam to spatially varying seismic excitation", *Earthquake Engineering and Structural Dynamics*, 1990, 19, pp. 173-187.

[10] Zerva, A., "Response of multi-span beams to spatially incoherent seismic ground motion", *Earthquake Engineering and Structural Dynamics*, 1990, 19, pp. 819-832.

[11] Kiureghian, A.D., Neuenhofer, A. "Response spectrum method for multiple-support seismic excitation", *Earthquake Engineering and Structural Dynamics*, 1992, 21, pp. 713-740.

[12] Zavoni, H., Vanmarcke, E.H., "Random-vibration based response spectrum method for multi-support structural systems", *Journal of Seismology and Earthquake Engineering*, 1998, 1, pp. 35-50.

[13] Sarkar, A., Manohar, C.S., "Critical cross power spectral density functions and the highest response of multi-supported structures to multi component earthquake excitations", *Earthquake Engineering and Structural Dynamics*, 1996, 25, pp. 303-315.

[14] Sarkar, A., Manohar, C.S., "Critical seismic vector random excitations for multi-supported structures", *Journal of Sound and Vibration*, 1998, 212, pp. 525-546.

[15] Abbas, A.M., Manohar, C.S., "Investigations into critical earthquake load models within deterministic and probabilistic frameworks", *Earthquake Engineering and Structural Dynamics*, 2002, 31, pp. 813-832.

[16] Clough, R.H., Penzien, J., "*Dynamics of structures*", McGraw-Hill, 2nd edition, Tokyo, 1993.

[17] Abbas, A.M., "*Deterministic/reliability-based critical earthquake load models for linear/nonlinear engineering structures*", Ph. D. thesis, Department of Civil Engineering, Indian Institute of Science, February 2002.

Case	Constraints imposed		
	Model I	Model II	Model III
1	Energy & PGA	$0 \leq \lvert S_{jl}(\omega)\rvert \leq \sqrt{S_{jj}(\omega)S_{ll}(\omega)}$, Phase known	Energy & PGA
2	Energy, PGA & PGV, PGD	$0 \leq \lvert S_{jl}(\omega)\rvert \leq \sqrt{S_{jj}(\omega)S_{ll}(\omega)}$, Phase unknown	Energy, PGA, PGV & PGD
3	Energy, PGA, PGV* & UBFAS	-	-
4	Energy, PGA, PGV*, UBFAS & LBFAS	-	-

Table 1: Nomenclature combinations of constraints used for Model I: Deterministic model of section 2; Model II: Probabilistic model of section 3 and Model III: Data base model of section 4; response variable is dynamic component, * PGV is replaced by PGD when response variable is pseudo-static component

Response variable	Model I, case 4			Model II, case 1			Model III, case 2		
	$u_{\max}$ (m)	$BM_{\max}$ (kN m)	$SF_{\max}$ (kN)	$\sigma_{u_{\max}}$ (m)	$\sigma_{BM_{\max}}$ (kN m)	$\sigma_{SF_{\max}}$ (kN)	$u_{\max}$ (m)	$BM_{\max}$ (kN m)	$SF_{\max}$ (kN)
Displacement	0.0199	12.5803	0.2536	0.0062	6.3498	0.1361	0.0237	15.9738	0.2636
Bending moment	0.0189	13.1705	0.2499	0.0053	7.6215	0.1372	0.0224	18.5168	0.2696
Shear force	0.0194	11.8823	0.2768	0.0051	6.7134	0.1451	0.0215	16.9330	0.3309

Table 2: Maximum dynamic responses for alternative critical response variables; objective function is the dynamic component

Response variable	Model I, case 4			Model II, case 1			Model III, case 2		
	$u_{s_{\max}}$ (m)	$BM_{s_{\max}}$ (kN m)	$SF_{s_{\max}}$ (kN)	$\sigma_{u_{s_{\max}}}$ (m)	$\sigma_{BMs_{\max}}$ (kN m)	$\sigma_{SFs_{\max}}$ (kN)	$u_{s_{\max}}$ (m)	$BM_{s_{\max}}$ (kN m)	$SF_{s_{\max}}$ (kN)
Displacement	0.1725	5350.2228	4285.9959	0.1142	2388.1571	1824.4542	0.1852	5355.8471	4289.3948
Bending moment	0.1672	5361.3253	4283.9457	0.0975	2411.5623	1839.7631	0.1792	5372.2182	4284.6571
Shear force	0.1641	5351.7428	4302.5632	0.0963	2397.4273	1848.2247	0.1695	5351.7623	4307.2341

Table 3: Maximum pseudo-static responses for alternative critical response variables; objective function is the pseudo-static component

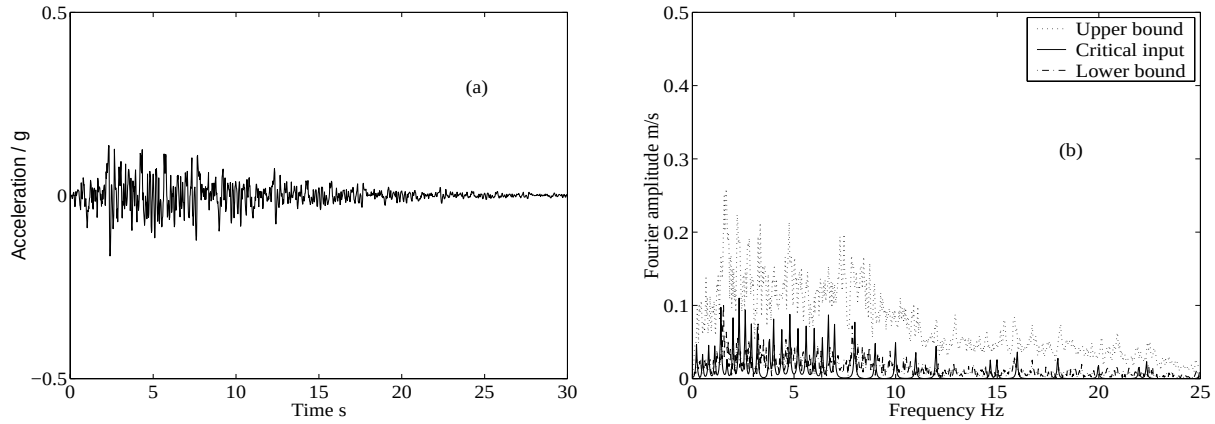

Figure 2: Model I, case 4: Critical acceleration at left support; (a) Time history (b) Fourier amplitude spectrum; response variable is $u_s(t)$ at the midpoint of left span

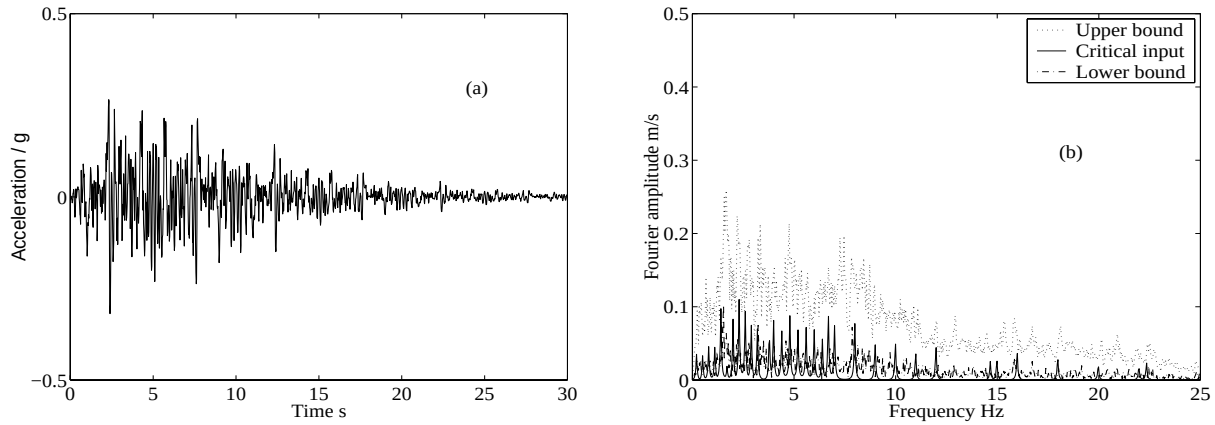

Figure 3: Model I, case 4: Critical acceleration at middle support; (a) Time history (b) Fourier amplitude spectrum ; response variable is $u_s(t)$ at the midpoint of left span

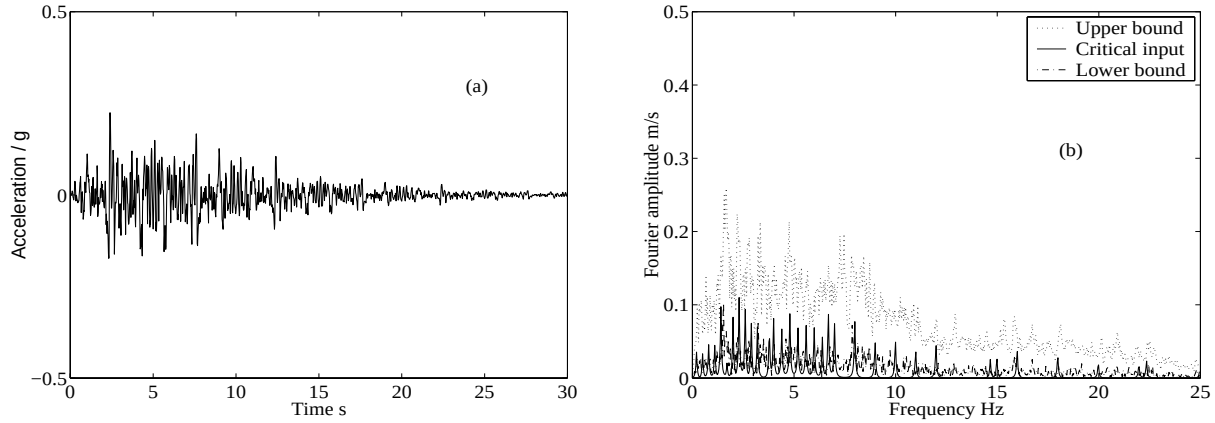

Figure 4: Model I, case 4: Critical acceleration at right support; (a) Time history (b) Fourier amplitude spectrum; response variable is $u_s(t)$ at the midpoint of left span

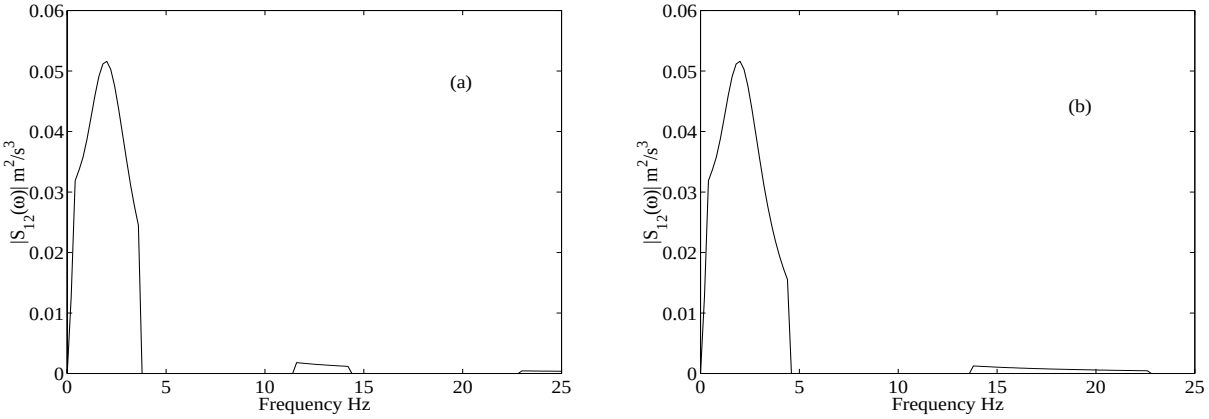

Figure 5: Model II, case 1: Critical $|S_{12}(\omega)|$ (a) response variable is $\sigma^2_{BM}(t)$ at the midpoint of left span (b) response variable is $\sigma^2_{BM_s}(t)$ at middle support

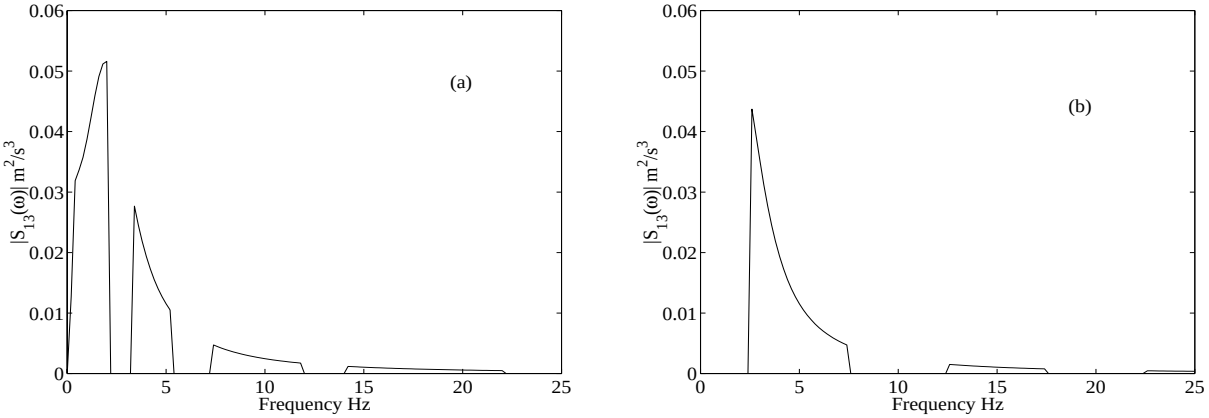

Figure 6: Model II, case 1: Critical $|S_{13}(\omega)|$ (a) response variable is $\sigma^2_{BM}(t)$ at the midpoint of left span (b) response variable is $\sigma^2_{BM_s}(t)$ at middle support

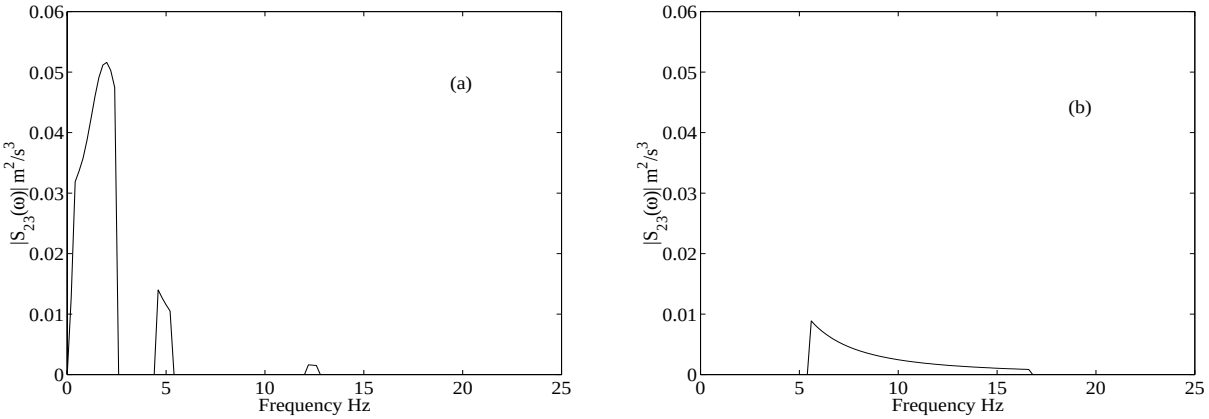

Figure 7: Model II, case 1: Critical $|S_{23}(\omega)|$ (a) response variable is $\sigma^2_{BM}(t)$ at the midpoint of left span (b) response variable is $\sigma^2_{BM_s}(t)$ at middle support

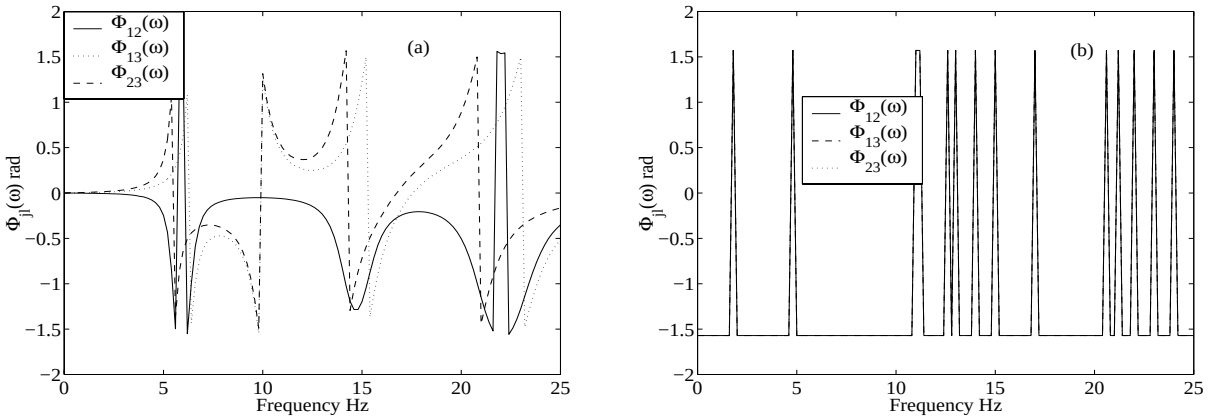

Figure 8: Model II, case 2: Critical $\Phi_{jl}(\omega)$; (a) response variable is $\sigma_u^2(t)$ at the midpoint of left span (b) response variable is $\sigma_{u_s}^2(t)$ at the midpoint of left span

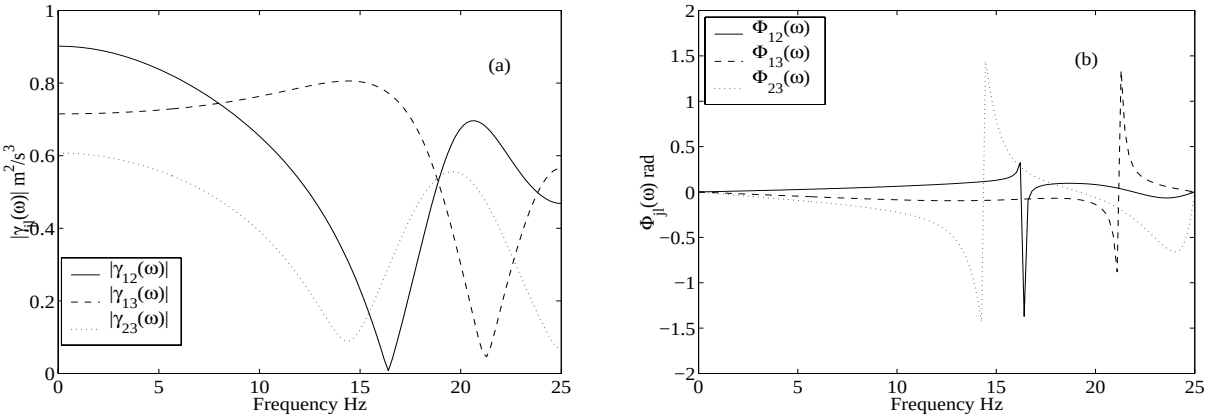

Figure 9: Model I, case 4: Coherency functions of ground accelerations; (a) $|\gamma_{jl}(\omega)|$ (b) $\Phi_{jl}(\omega)$; response variable is $\sigma_u^2(t)$ at the midpoint of left span

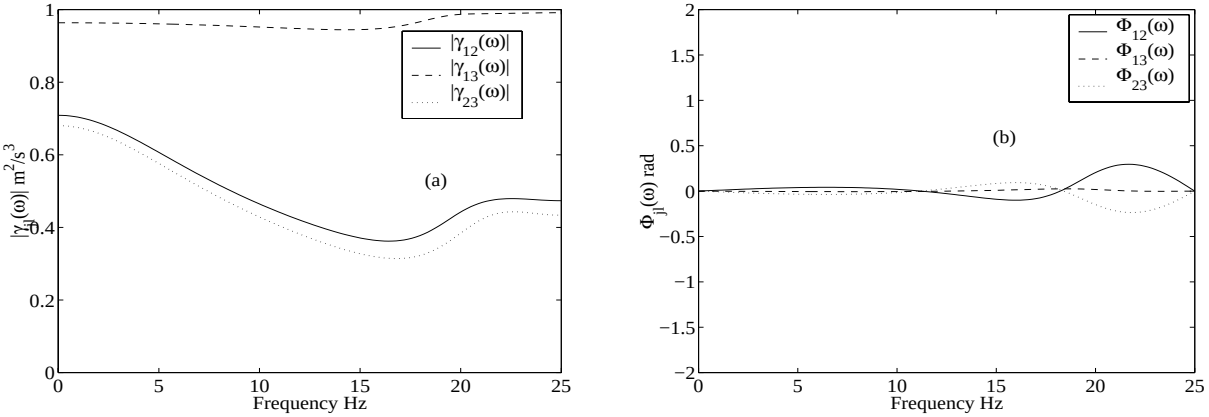

Figure 10: Model I, case 4: Coherency functions of ground accelerations; (a) $|\gamma_{jl}(\omega)|$ (b) $\Phi_{jl}(\omega)$; response variable is $\sigma_{u_s}^2(t)$ at the midpoint of left span